

## **FLEXIBLE UNIPLANAR ARTIFICIAL MAGNETIC CONDUCTOR**

**M. E. de Cos, Y. Álvarez, R. Hadarig, and F. Las-Heras**

Área de Teoría de la Señal y Comunicaciones  
Departamento de Ingeniería Eléctrica  
Universidad de Oviedo  
Edificio Polivalente, Modulo 8, Campus Universitario de Gijón  
E-33203Gijón, Asturias, Spain

**Abstract**—The design of a flexible uniplanar AMC is presented. A prototype is manufactured and characterized based on reflection coefficient phase under flat and bent conditions. The designed prototype shows broad AMC operation bandwidth and polarization angle independency in both flat and bent situations. Its angular margin when operating under oblique incidence is also tested. FEM simulations and measurements in an anechoic chamber are presented.

### **1. INTRODUCTION**

In recent years, artificial magnetic conductor (AMC) structures composed of composite materials or circuit components [1, 2], are widely studied due to their unique properties in controlling the propagation of electromagnetic waves, which makes them a promising alternative to face antennas and microwaves circuits' problems.

AMCs are synthesized Perfect Magnetic Conductors (PMCs) (as these do not exist in nature) and are dual to a Perfect Electric Conductor (PEC) from an electromagnetic point of view. In the ideal lossless case, AMC condition is indicated by a reflection coefficient with a magnitude value of 1 and a phase value of  $0^\circ$ . However, it is considered [1–3] that AMCs behave as PMCs over a certain frequency band, the so called bandwidth of AMC performance or AMC operation bandwidth, which is generally defined in the range from  $+90^\circ$  to  $-90^\circ$ , since in this range, the phase values would not cause destructive interference between direct and reflected waves.

---

*Received 15 June 2010, Accepted 20 July 2010, Scheduled 26 July 2010*

Corresponding author: M. E. de Cos (cosmaria@uniovi.es).

One of the more extensively used AMCs' implementation techniques consists in using two-dimensional periodic metallic lattices patterned on a conductor-backed dielectric surface, also called electromagnetic band-gap (EBG) surfaces [16–19], as they have one or multiple frequency bandgaps in which no substrate mode can exist [3]. Enhanced in gain and efficiency, antennas with low back lobe and low side lobe level [20–33] should be mentioned between the most fructiferous EBGs' applications. Other applications involve filters [34–41], power amplifiers [44] and absorbing screens [42].

Recent research efforts focus on the development of low-cost AMCs that can be easily integrated in microwave and millimeterwave circuits. This means, on one hand, the use of EBGs without via holes [2, 4–8] (in contrast to designs consisting in patches with via holes [1, 10]) and, on the other hand, the use of an unilayer periodic Frequency Selective Surface (FSS) over a metallic ground plane (in contrast to multilayered FSSs [15]). The main limitation in the unilayer case is the very narrow AMC operation bandwidth, due to EBGs' inherent resonant nature. However, this can be compensated, to some extent, with an optimized unit cell geometry design and the use of relatively low relative dielectric permittivity substrates, which in addition reduces the cost.

In some of the AMCs' prospect applications, such as its use in Radio Frequency Identification (RFID) tags over metallic objects [6], wearable antennas [11–14] and RCS reduction [42, 43], it would be desirable to have the AMC object-shape-adapted. This would require the AMC to be flexible (especially in the case of objects with curved surfaces) but without losing its functionality. Thus it is interesting to analyze flexible AMCs' performance.

In this contribution, the novel AMC design with neither via holes nor multilayer substrates presented in [9] is manufactured using a bendable dielectric substrate, which adds the advantage of flexibility to the resulting AMC structure, preserving the design features remarked in [9]: planar feature, compact size, low dielectric losses and broad AMC operation bandwidth, as it will be shown in the section II. In this way, a flexible AMC which meets the reduced-cost and easy-to-manufacture-and-integrate requirements is obtained.

## 2. PLANAR AMC DESIGN

The resonance frequency and the bandwidth of an AMC design depend on the unit cell geometry together with substrate's relative dielectric permittivity and thickness. In [9], a trade-off solution regarding substrate's relative dielectric permittivity is adopted in order to obtain both compact size and broad AMC operation bandwidth.

The PMC behavior characteristics of a FSS surface over a metallic ground plane can be verified by simulating the reflection coefficient for a uniform incident plane wave. So, to search for the frequency band in which the periodic structure behaves as an AMC, a Finite Element Method (FEM) simulation based on the Bloch-Floquet theory is considered, modeling a single cell of the structure with periodic boundary conditions (PBC) on its four sides, resembling the modeling of an infinite structure.

The designed unit cell geometry of [9] is shown in Fig. 1(a). Arlon 25 N, with relative dielectric permittivity,  $\epsilon_r = 3.28$ , loss tangent less than 0.0025 and a thickness of  $h = 0.762$  mm (30 mils), is used as dielectric substrate. Unit cell dimensions are  $W \times W = 11.52$  mm  $\times$  11.52 mm and its geometry exhibits four symmetry planes. The metallization thickness is 18  $\mu$ m. Such dimensions resulted in an AMC operating in the 5.8 GHz band: for the  $12 \times 12$  cells planar AMC manufactured prototype shown in Fig. 1(b) the resonance frequency is 5.89 GHz and the frequency bandwidth of AMC performance is approximately 433 MHz (7.3%).

In this contribution, the same unit cell design of [9] is going to be used, but with a different dielectric substrate, RO3003 of Rogers, which is bendable and has the same thickness ( $h = 0.762$  mm (30 mils)), a slightly lower relative dielectric permittivity ( $\epsilon_r = 3.0$ ) and loss tangent (0.0013). For the same unit cell size a slight shift to a higher resonance frequency would be expected, due to the reduction in the relative dielectric permittivity. If the resonance frequency is desired to be kept in the 5.8 GHz band (for example to be used for an RFID tag) using RO3003 with 30 mils thickness, the unit cell size has to be slightly increased by using a 1.05 scale factor as shown in Fig. 2.

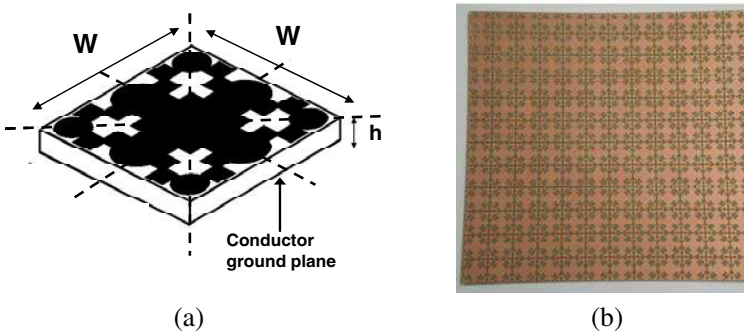


**Figure 1.** Unit cell geometry. (a) Side view, (b) planar AMC manufactured prototype.

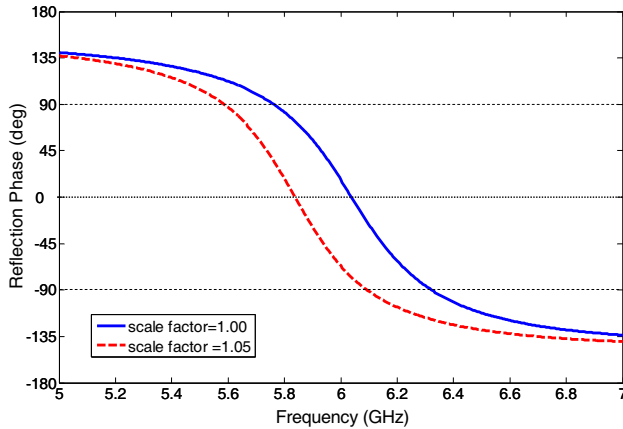


**Figure 2.** Reflection phase shifting versus scale factor of unit cell of [9].

### 3. FLEXIBLE AMC CHARACTERIZATION

A  $12 \times 12$  cells planar AMC prototype has been manufactured using laser micromachining (see Fig. 1(b)) and it has been measured in order to validate the simulation results.

#### 3.1. Measurement Setup in Anechoic Chamber

Neither the measurement setup in anechoic chamber nor the methodology is changed with respect to the characterization of an AMC implemented on a rigid dielectric substrate.

Regarding the measurement setup (see Fig. 3) two horn antenna probes working in the band 5–7 GHz have been chosen as Tx and Rx being the separation between each probe and the object-under-test 5 m. The proposed measurement setup ensures that the scattered field is acquired in the far-field region, since accounting for the upper limit of the frequency band (7 GHz,  $\lambda = 4.28$  cm) and the object-under-test size ( $D = 13.82$  cm), far-field distance can be estimated as  $R_{FF} = 2D^2/\lambda = 0.89$  m.

With regards to the followed methodology [1], it is based on the utilization of a reference measurement (flat metallic plate) to calculate the reflection coefficient of the AMC substrate and is the same used for the full-wave simulation.

Accurate measurement of the reflection phase requires the measurement distance to be the same for both the metallic plate and the AMC prototype (having both the same size). In this case, the

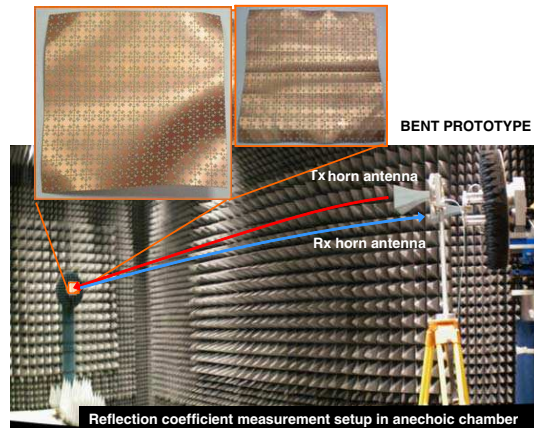


**Figure 3.** Reflection coefficient measurement setup in anechoic chamber.

flexible AMC has a bending depth of  $h$ , which causes the measurement distance to be different. However, the distance variation ( $h$ ) is negligible with respect to the measurement distance (5 m). The frequency shift due to a distance variation of  $h$  has been tested. The frequency shift is 4 MHz (0.06%) for  $h = 10$  mm which is the maximum bending depth of the flexible AMC prototypes.

In order to obtain the characterization results presented in the following sections (3.2, 3.3 and 3.4) measurements of the flat (i.e., not bent) AMC prototype have been firstly carried out. Then, the prototype has been bent (see Fig. 3 and Fig. 5) and measured.

### 3.2. Reflection Phase Measurement for AMC Band Determination

A flexible AMC can be bent in many arbitrary ways. Between the multiple possible ways of bending, two typical different possibilities have been selected and tested (see Fig. 5): A “creeping” pattern (henceforth referred as creeping prototype) and a “smooth” pattern (henceforth referred as smooth prototype). The ratio between the minimum bending radius of curvature and the AMC unit cell size is 0.43 for the creeping prototype and 0.86 for the smooth prototype. This minimum bending radius of curvature corresponds to  $0.1\lambda$  for the creeping prototype and  $0.21\lambda$  for the smooth prototype.

In Fig. 4, the measured reflection phase of the flat and bent manufactured prototypes is represented together with the flat AMC structure simulation results for normal incidence conditions. Regarding

the manufactured flat prototype, it has the resonance at 6.23 GHz which means a 3.3% deviation with respect to the simulation (6.03 GHz). The cause of this shift between the measured AMC resonance frequency and the simulated value is typically attributable to the manufacturing process as justified in [45] due to under-etching in the laser micromachining. However, there is no frequency shift for the manufactured creeping bent prototype with respect to the flat prototype resonance, whereas the smooth bent prototype has its resonance at 6.27 GHz, which means just a 0.6% deviation with respect to the flat prototype.

The frequency bandwidth of AMC performance for the flat prototype is 392 MHz (6.29%) in good agreement with simulated value (7.84%) (see Fig. 4) whereas for the creeping bent prototype the bandwidth of AMC performance is 387 MHz (6.19%) and for the smooth bent AMC is 416 MHz (6.63%), even slightly greater than that of the flat prototype.

As the behaviour of the smooth prototype presents a slight frequency shift and variation in the bandwidth of AMC performance with respect to the flat prototype, the influence of the incident field polarization angle and the angular stability under oblique incidence have been analyzed for this prototype, taking advantage of the measurement setup capabilities, and are described in the next subsections.

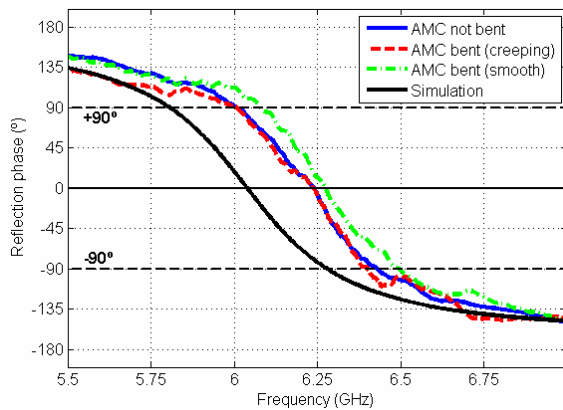


**Figure 4.** Reflection phase of the flat (simulated and measured) and bent (measured) prototypes.

### 3.3. Reflection Phase Characterization for Different Field Polarization Angles

The reflection phase of the manufactured AMC prototypes has been measured for different incident field polarization angles ( $\varphi$ ).

The unit cell design symmetry makes possible the AMC to operate identically for any polarization of the incident field (assuming normal incidence) for the flat prototype. This behaviour remains for the smooth bent prototype, as shown in Fig. 6.

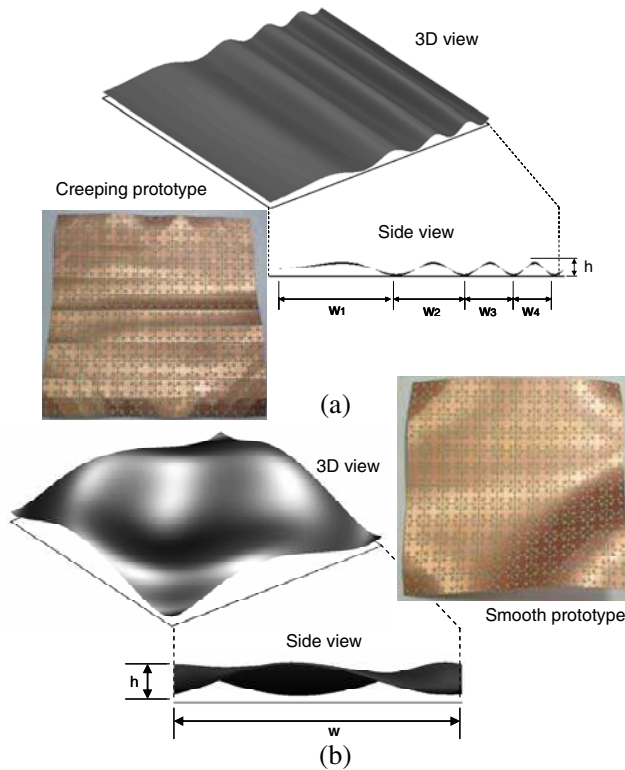


**Figure 5.** Bending patterns. (a) Creeping prototype with  $W_1 = 56.6$  mm,  $W_2 = 30.0$  mm,  $W_3 = 21.5$  mm,  $W_4 = 18.3$  mm and  $h = 5$  mm, (b) smooth prototype with  $W = 120$  mm, and  $h = 10$  mm.

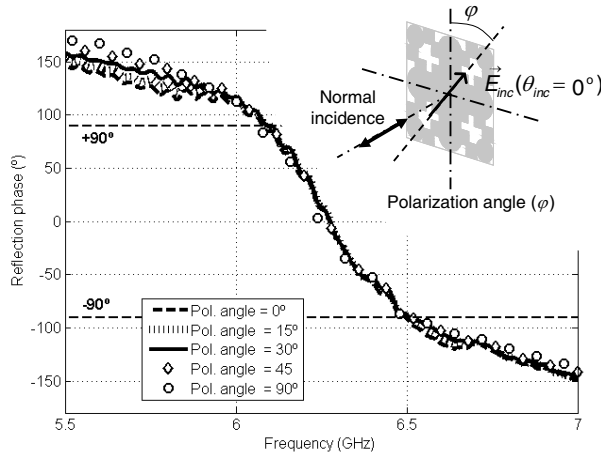


**Figure 6.** Reflection phase of the manufactured smooth prototype for different incident field ( $E_{inc}$ ) polarization angles ( $\varphi$ ).

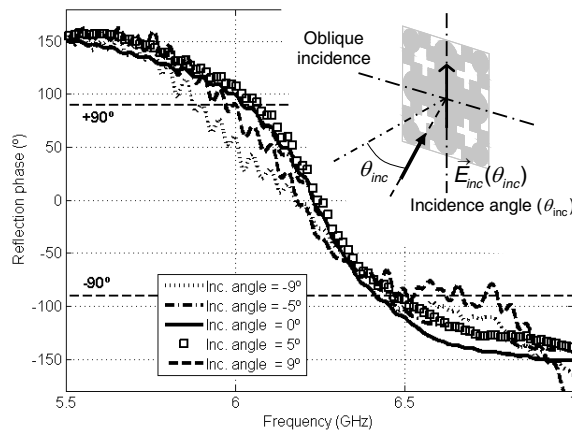


**Figure 7.** Reflection phase of the manufactured AMC surface for different incident angles ( $\theta_{inc}$ ) when the AMC is flat.

### 3.4. Reflection Phase Characterization for Different Incidence Angles

To obtain comprehensive information about the angular stability margin of the presented structure both in flat and smooth bent conditions, the reflection coefficient phase versus frequency, for different incident angles  $\theta_{inc}$  has been measured. Resonance conditions

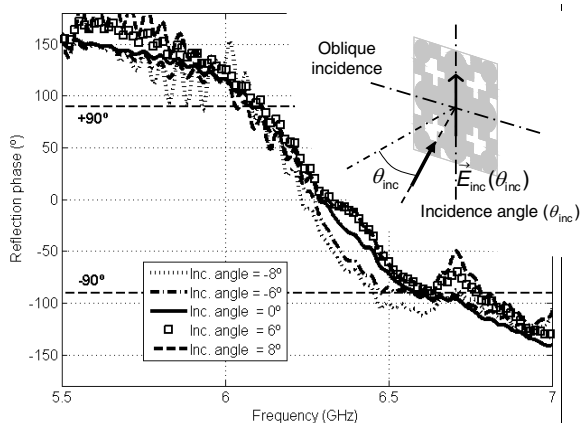


**Figure 8.** Reflection phase of the manufactured smooth prototype for different incident angles ( $\theta_{inc}$ ).

are met within an angular margin of  $\theta_{inc} = \pm 9^\circ$  for the flat prototype (see Fig. 7) whereas the obtained angular margin is  $\theta_{inc} = \pm 8^\circ$  (see Fig. 8) for the smooth bent prototype.

#### 4. CONCLUSIONS

It is possible to obtain a flexible AMC hardly (or even without) reducing the bandwidth of AMC performance with respect to a rigid AMC that uses the same unit cell design. A prototype based on a novel uniplanar AMC has been manufactured using a thin and low relative dielectric permittivity commercial substrate, and it has been characterized, based on reflection coefficient phase, under flat and bent conditions, using two different bending patterns. It shows polarization angle-independency under normal incidence and hardly reduces its angular margin when operating under oblique incidence.

The absence of via holes and the uniplanar geometry characteristics of the presented design together with the flexible characteristic make it very attractive for applications regarding antennas in RFID tags and Wearable systems, and also as part of Microwave Integrated Circuits (MICs) and Monolithic Microwave Integrated Circuits (MMICs) due to its simple fabrication and integration, and low cost.

## ACKNOWLEDGMENT

This work has been supported by the “Ministerio de Ciencia e Innovación” of Spain/FEDER” under projects TEC2008-01638/TEC (INVENTA) and CONSOLIDER CSD2008-00068 (TERASENSE), by PCTI Asturias under project, PEST08-02 (MATID) and by the Principado de Asturias/FEDER Project IB09-081 (CAMSILOC).

## REFERENCES

1. Sievenpiper, D., et al., “High-impedance electromagnetic surfaces with a forbidden frequency band,” *IEEE Trans. Microwave Theory Tech.*, Vol. 47, No. 11, 2059–2074, Nov. 1999.
2. Yang, F. R., K. P. Ma, Y. Qian, and T. Itoh, “A uniplanar compact photonic-bandgap (UC-PBG) structure and its applications for microwave circuit,” *IEEE Trans. Microwave Theory Tech.*, Vol. 47, No. 8, 1509–1514, 1999.
3. Yang, F. and Y. Rahmat-Samii, “Electromagnetic band-gap structures in antenna engineering,” *The Cambridge RF and Microwave Engineering Series*, Cambridge University Press, 2008.
4. McVay, J., N. Engheta, and A. Hoofar, “High impedance metamaterials surfaces using Hilbert-curve inclusions,” *IEEE Microw. Wire. Comp. Lett.*, Vol. 14, No. 3, 130–132, 2004.
5. Kim, Y., F. Yang, and A. Z. Elsherbeni, “Compact artificial magnetic conductor design using planar square spiral geometries,” *Progress In Electromagnetics Research*, Vol. 77, 43–54, 2007.
6. De Cos, M. E., F. Las-Heras, and M. Franco, “Design of planar artificial magnetic conductor ground plane using frequency-selective surfaces for frequencies below 1 GHz,” *IEEE Antennas and Wireless Propagation Letters*, Vol. 8, 951–954, 2009.
7. De Cos, M. E., Y. Álvarez, and F. Las-Heras, “Planar artificial magnetic conductor: Design and characterization setup in the RFID SHF band,” *Journal of Electromagnetic Waves and Applications*, Vol. 23, No. 11–12, 1467–1478, 2009.
8. Kern, D. J., D. H. Werner, A. Monorchio, L. Lanuza, and M. J. Wilhelm, “The design synthesis of multiband artificial magnetic conductors using high impedance frequency selective surfaces,” *IEEE Trans. on Antennas and Propag.*, Vol. 53, No. 1, Jan. 2005.
9. De Cos, M. E., Y. Álvarez, R. C. Hadarig, and F. Las-Heras, “Novel SHF band uniplanar Artificial Magnetic Conductor,”

- IEEE Antennas and Wireless Propagation Letters*, Vol. 9, 44–47, 2010.
10. Luukkonen, O., C. R. Simovski, and S. A. Tretyakov, “Grounded uniaxial material slabs as magnetic conductors,” *Progress In Electromagnetics Research B*, Vol. 15, 267–283, 2009.
  11. Zhu, S. and R. Langley, “Dual-band wearable textile antenna on an EBG substrate,” *IEEE Trans. on Antennas and Propag.*, Vol. 57, No. 4, Apr. 2009.
  12. Salonen, P. and Y. Rahmat-Samii, “Textile antennas: Effects of antenna bending on input matching and impedance bandwidth,” *IEEE Aerospace Electronic Systems Magazine*, Vol. 22, No. 3, 10–14, 2007.
  13. Salonen, P., M. Keskilammi, and L. Sydanheimo, “A low-cost 2.45 GHz photonic band-gap patch antenna for wearable systems,” *Proc. 11th Int. Conf. Antennas and Propagation*, 719–724, Apr. 17–20, 2001.
  14. Salonen, P. and Y. Rahmat-Samii, “WEBGA-wearable electromagnetic band-gap antenna,” *IEEE APS Int. Symp. Dig.*, Vol. 1, 451–454, Monterrey, CA, Jun. 2004.
  15. Monorchio, A., G. Manara, and L. Lanuzza, “Synthesis of artificial magnetic conductors by using multilayered frequency selective surfaces,” *IEEE Ant. Wireless Propag. Lett.*, Vol. 1, 196–199, 2002.
  16. Xie, H.-H., Y.-C. Jiao, K. Song, and Z. Zhang, “A novel multi-band electromagnetic band-gap structure,” *Progress In Electromagnetics Research Letters*, Vol. 9, 67–74, 2009.
  17. Srivastava, R., K. B. Thapa, S. Pati, and S. P. Ojha, “Omnidirectional reflection in one dimensional photonic crystal,” *Progress In Electromagnetics Research B*, Vol. 7, 133–143, 2008.
  18. Ekmekci, E. and G. Turhan-Sayan, “Comparative investigation of resonance characteristics and electrical size of the double-sided Srr, Bc-Srr and conventional srr type metamaterials for varying substrate parameters,” *Progress In Electromagnetics Research B*, Vol. 12, 35–62, 2009.
  19. Pajewski, L., L. Rinaldi, and G. Schettini, “Enhancement of directivity using 2D-electromagnetic crystals near the band-gap edge: A full-wave approach,” *Progress In Electromagnetics Research*, Vol. 80, 179–196, 2008.
  20. Yang, F. and Y. Rahmat-Samii, “Reflection phase characterizations of the EBG ground plane for low profile wire antenna applications,” *IEEE Trans. on Antennas and Propag.*, Vol. 51, No. 10,

- 2691–2701, 2003.
21. McVay, J., A. Hoofar, and N. Engheta, “Small dipole-antenna near Peano high-impedance surfaces,” *IEEE AP-S Int. Symp.*, Vol. 1, 305–308, 2004.
  22. Mosallaei, H. and K. Sarabandi, “Antenna miniaturization and bandwidth enhancement using a reactive impedance substrate,” *IEEE Trans. on Antennas and Propag.*, Vol. 52, No. 9, Sep. 2004.
  23. Akhoondzadeh-Asl, L., D. J. Kern, P. Hall, and D. Werner, “Wideband dipoles on electromagnetic bandgap ground planes,” *IEEE Trans. on Antennas and Propag.*, Vol. 55, No. 9, Sep. 2007.
  24. Liang, J. and H.-Y. D. Yang, “Radiation characteristics of a microstrip patch over an electromagnetic bandgap surface,” *IEEE Trans. on Antennas and Propag.*, Vol. 55, No. 6, Jun. 2007.
  25. Feresidis, A. P., G. Goussetis, S. Wang, and J. C. Vardaxoglou, “Artificial magnetic conductor surfaces and their application to low profile highgain planar antennas,” *IEEE Trans. on Antennas and Propag.*, Vol. 53, No. 1, 209–215, Jan. 2005.
  26. Sohn, J. R., K. Y. Kim, and H.-S. Tae, “Comparative study on various artificial magnetic conductors for low-profile antenna,” *Progress In Electromagnetics Research*, Vol. 61, 27–37, 2006.
  27. Yang, F. and Y. Rahmat Samii, “Reflection phase characterizations of the EBG ground plane for low profile wire antenna,” *Progress In Electromagnetics Research*, Vol. 77, 2007.
  28. Shaban, H., H. Elmikaty, and A. A. Shaalan, “Study the effects of electromagnetic band-gap (EBG) substrate on two patch microstrip antenna,” *Progress In Electromagnetics Research B*, Vol. 10, 55–74, 2008.
  29. Hosseini, M. and S. Bashir, “A novel circularly polarized antenna based on an artificial ground plane,” *Progress In Electromagnetics Research Letters*, Vol. 5, 13–22, 2008.
  30. Pirhadi, A., F. Keshmiri, M. Hakkak, and M. Tayarani, “Analysis and design of dual band high directive EBG resonator antenna using square loop FSS as superstrate layer,” *Progress In Electromagnetics Research*, Vol. 70, 1–20, 2007.
  31. Rajo-Iglesias, E., L. Inclán-Sánchez, and O. Quevedo-Teruel, “Back radiation reduction in patch antennas using planar soft surfaces,” *Progress In Electromagnetics Research Letters*, Vol. 6, 123–130, 2009.
  32. Yuan, H.-W., S.-X. Gong, X. Wang, and W.-T. Wang, “Scattering analysis of a printed dipole antenna using PBG structures,” *Progress In Electromagnetics Research B*, Vol. 1, 189–195, 2008.

33. Duan, Z., S. Qu, and Y. Hou, "Electrically small antenna inspired by spired split ring resonator," *Progress In Electromagnetics Research Letters*, Vol. 7, 47–57, 2009.
34. Moghadasi, S. M., A. R. Attari, and M. M. Mirsalehi, "Compact and wideband 1-D mushroom-like EBG filters," *Progress In Electromagnetics Research*, Vol. 83, 323–333, 2008.
35. Srivastava, R., K. B. Thapa, S. Pati, and S. P. Ojha, "Design of photonic band gap filter," *Progress In Electromagnetics Research*, Vol. 81, 225–235, 2008.
36. Fallahzadeh, S., H. Bahrami, and M. Tayarani, "A novel dual-band bandstop waveguide filter using split ring resonators," *Progress In Electromagnetics Research Letters*, Vol. 12, 133–139, 2009.
37. Awasthi, S. K., U. Malaviya, S. P. Ojha, N. K. Mishra, and B. Singh, "Design of a tunable polarizer using a one-dimensional nano sized photonic bandgap structure," *Progress In Electromagnetics Research B*, Vol. 5, 133–152, 2008.
38. Hu, X., Q. Zhang, and S. He, "Compact dual-band rejection filter based on complementary meander line split ring resonator," *Progress In Electromagnetics Research Letters*, Vol. 8, 181–190, 2009.
39. Liu, J.-C., H.-C. Lin, and B.-H. Zeng, "Complementary split ring resonators with dual mesh-shaped couplings and defected ground structures for wide pass-band and stop-band BPF design," *Progress In Electromagnetics Research Letters*, Vol. 10, 19–28, 2009.
40. Karthikeyan, S. S. and R. S. Kshetrimayum, "Compact wideband bandpass filter using open slot split ring resonator and CMRC," *Progress In Electromagnetics Research Letters*, Vol. 10, 39–48, 2009.
41. Hsu, H., M. J. Hill, R. W. Ziolkowski, and J. Papapolymou, "A duroid-based planar EBG cavity resonator filter with improved quality factor," *IEEE Antennas and Propag. Letters*, Vol. 1, 67–70, 2002.
42. Engheta, N., "Thin absorbing screens using metamaterial surfaces," *IEEE Antennas and Propag. Society International Symp.*, Vol. 2, 392–395, Jun. 16–21, 2002.
43. Zheng, Q.-R., Y.-M. Yan, X.-Y. Cao, and N.-C. Yuan, "High impedance ground plane (Higp) incorporated with resistance for radar cross section (RCS) reduction of antenna," *Progress In Electromagnetics Research*, Vol. 84, 307–319, 2008.

44. Belaid, M. and K. Wu, "Spatial power amplifier using a passive active TEM waveguide concept," *IEEE Trans. Microwave Theory and Tech.*, Vol. 51, No. 3, 684–689, Mar. 2003.
45. Li, Y. D., et al., "Prototyping dual-band artificial magnetic conductors with laser micromachining," *Proc. of WARS Conference*, Leura, NSW, Australia, Feb. 2006.